2.1 Introduction

This chapter describes the common experimental protocols adopted for the synthesis and catalytic studies of Ag, Cu, Ag-Cu BNPs and reduced graphene oxide supported Ag/rGO, Cu/rGO and Ag-Cu/rGO BNPs. The experimental methodology used to evaluate the catalytic performance of synthesized nanomaterials for model reactions such as Nip reduction and MO oxidation is also stated. Thereafter, the experimental procedure used for recording the photocatalytic activity of these nanocatalysts is presented. Finally, the details of the working principles of an instrument is being utilized for the chemical and structural characterization of synthesized nanomaterials and the products formed after catalysis are given.

2.2 Chemicals

All chemicals utilized in the synthesis and catalytic studies carried out in this thesis were of analytical grade and used without further purification. Distilled water of ~ 6.8 pH was used in both for the synthesis and catalytic studies of the present work. Specifications of the chemicals used in the experiments studies are presented in the Table 2.1.

Table 2.1 Details of chemicals like name, chemical formula, molecular weight, physical appearance and manufacturer name of the reagent used in present work.

Sr. No.	Chemical name	Chemical formula	Molecular weight (g)	Manufacturer	Appearance
1	Silver nitrate	$Ag(NO_3)$	169.87	Merk	White crystal
2	Copper nitrate	$Cu(NO_3)_2$	241.60	Merk	Blue Crystal
3	Copper acetate	$Cu(OCH_3)_2$	199.65	Merck	Greenish blue crystal
4	Curcumin	$C_{21}H_{20}O_6$	368.39	Sigma Aldrich	Yellow powder
5	Poly-vinylpyrrolidone	$(C_6H_9NO)_n$	40,000	Himedia	White powder
6	Ethylene glycol	$C_2H_6O_2$	62	Mecrk	Colorless liquid
7	Sodium hydroxide	NaOH	40	Merck	White Pellet
8	Hydrazine hydrate	N_2H_4	18	Merck	Colorless liquid
9	p-nitrophenol	$C_6H_5NO_3$	139.11	Spectrochem	Yellow Solid
10	Sodium borohydride	$NaBH_4$	37.83	Molychem	White powder
11	Methyl orange	$C_{14}H_{14}N_3NaO_3S$	327.33	Molychem	Orange powder
12	Hydrogen peroxide	H_2O_2	34.01	Merck	Colorless liquid
13	Ammonia	NH_3	17.01	Merck	Colorless liquid

2.3 Synthesis and catalytic experiments of Ag, Cu and Ag-Cu BNPs

Ag, Cu, Ag-Cu BNPs and Ag/rGO, Cu/rGO, Ag-Cu/rGO BNPs are synthesized by liquid phase chemical reduction methodologies. Chemical reduction method is most likely the most efficient chemical pathway to achieve Ag and Cu nanoparticles. The bimetallic nanoparticles are prepared by the reduction of stoichiometric ratios of silver and copper salts in presence of different stabilizers. Liquid phase chemical reduction synthesis of these nanoparticles is a combination of reduction, nucleation and growth followed by aggregation. The relatively higher reduction potential of $Ag^+ \rightarrow Ag^0$ in water (E_0 = + 0.80

eV) permits the use of strong as well as weak reducing agents for reducing Ag^+ ions. But for $Cu^{2+} \rightarrow Cu^0$ reduction the reduction potential (E_0 = + 0.34 eV) is lesser, and therefore stronger reducing agents such as hydrazine hydrate, $NaBH_4$, etc. are needed. In this work copper ions were reduced with hydrazine hydrate.

2.4 Thermal catalytic reduction of Nip and oxidation of MO

2.4.1 Catalytic reduction of Nip with $NaBH_4$

For this study, 0.1 mL of 1.2×10^{-3} M Nip solution was diluted by adding 1.85 mL water and taken in a standard quartz cuvette of 1 cm path length. To this 50 µL of aqueous 0.1 M $NaBH_4$ was added. For the blank experiment (without catalyst) the UV-visible spectrum of this reaction mixture was monitored at regular intervals for about 70 minutes. Next, the actual experiment was carried out in presence of catalyst and the absorption spectrum recorded at regular intervals. The above procedure was repeated to monitor the kinetics of the catalyzed reaction at four different temperatures. Experiments at each temperature were repeated appropriate number of times to generate error bars.

2.4.2 Catalytic reduction of Nip with glycerol

For this purpose, 2 mL of 2.67 M glycerol solution was taken in a standard quartz cuvette of 1 cm path length. To this 0.1 mL of $1.2x10^{-3}$ M Nip solution was added. Then appropriate amount 0.1 M NaOH solution was added to the above reaction mixture such that the pH of solution turns basic (~ 8.5). First, the blank experiment, without catalyst, was done. Then, the actual experiment in presence of the catalyst was carried out. The absorption spectrum of this reaction mixture was recorded at regular time intervals. The same procedure was repeated to monitor the kinetics of catalyzed reaction at four different

temperatures. Experiments at each temperature were repeated three times to generate error bars.

2.4.3 Catalytic MO oxidation

For this, 0.14 mmol of MO was taken in a standard quartz cuvette of 1 cm path length. This was then diluted by 2 mL of water. Then the pH of this solution was adjusted to 3 (acidic) by using 0.1 N HCl and 0.1 N NaOH. To this 0.1 mL of H_2O_2 solution was added. The blank reaction (in absence of catalyst was monitored by UV-vis spectrophotometer at regular time intervals. Then the reaction was carried out in presence of appropriate amount catalyst. The absorption spectrum was recorded after every 10-minutes time interval. The kinetics of the catalyzed reaction was monitored at four different temperatures (303, 308, 313 and 318 K) by the same procedure. Experiments at each temperature were repeated appropriate number of times to generate error bars.

2.5 Photocatalytic Nip reduction and MO oxidation

2.5.1 Design of photocatalytic chamber

Photocatalytic chamber was prepared in such a way, all the four sides of chamber is fixed with a 7 watt white LED (Philcon) each and one white LED of power 13 watt (Philcon) from the top of the box. The overall arrangement was such that the reaction mixture in four sided quartz cuvette was irradiated with approximately 940 watts/m^2. The power of irradiation was measured with solar power meter TM-206. The temperature of the reaction mixture in this condition was found to be 303 K.

2.5.2 Photocatalytic Nip reduction with glycerol

Again for this study, 2 mL of 2.67 M glycerol solution was taken in a standard quartz cuvette of 1cm path length. To this 0.1 mL of $1.2x10^{-3}$ M Nip solution was added. Then 0.1 M NaOH solution was added to the above reaction mixture so that the pH of solution turns basic (~ 8.5). In all cases, at first a blank (without catalyst) visible light photocatalytic experiment was carried out. Thereafter, the photocatalytic experiment in presence of the catalyst was done. In both cases, the temperature of the photocatalytic chamber was 303 K. The absorption spectrum of the reaction mixture was recorded after every five-minute time interval.

2.5.3 Photocatalytic MO oxidation

2 mL of $1.71x10^{-4}$ M MO solution was taken in a standard quartz cuvette (four sided) of 1cm path length. The pH of this solution was then adjusted to ~ 3.0 with the help of few drops of 0.1 M HCl and 0.1 M NaOH solution. To this 0.1 mL of 50 mM H_2O_2 solution was added. The blank experiment (in absence of catalyst) was carried out under visible light irradiation in the photocatalytic chamber. The absorption spectrum of the reaction mixture was recorded at every five-minute time interval. Then, the experiment was carried out in presence of the catalyst and its absorption spectrum monitored in 200 to 700 nm range at regular intervals of time.

2.6 Techniques used for characterization of synthesized catalyst

Details of the characterization tools used are discussed in this section. The prepared nanoparticles were characterized by UV-visible spectroscopy, X-ray diffraction (XRD), Fourier transform infrared spectroscopy (FTIR), Nuclear magnetic resonance spectroscopy (NMR), Transmission electron microscopy (TEM) and High resolution scanning electron microscopy (HR-SEM). The LSPR characteristics of prepared noble metal nanoparticles

provide important information about the possible nanostructure formed. XRD is used to identify the phases formed. Fourier transform infrared spectroscopy was helpful in identifying different functional groups present on the surface of nanoparticles due to the presence of stabilizers. The product of the catalytic reaction was confirmed with the help of ^{1}HNMR spectroscopy. Shape and size of nanoparticles are obtained with the help of imaging of nanoparticles in transmission electron microscopy (TEM). Composition and presence of both the metals in bimetallic nanoparticles was further confirmed by elemental mapping with the help of HR-SEM.

2.6.1 UV-Visible spectrophotometer

Ultraviolet–visible absorption spectroscopic measurements were conducted on Agilent Cary 60 spectrophotometer. The sample environment was thermo-regulated by a thermostat (Peltier Cary 60). The Agilent Cary 60 model uses two light sources. The source utilized are, deuterium or hydrogen discharge tube for covering the UV region (200-370 nm) and a tungsten lamp for scanning the visible region (325-770 nm). Appropriately diluted sample was taken in a quartz cuvette of 1 cm path length for UV-vis measurement.

Principle

Electronic transitions of the molecule occur by the absorption of light in the UV-visible region. Molecules absorb ultraviolet or visible light (of frequency (υ) or wavelength (λ)) resulting in the transition of an electron from a lower to higher energy level in the molecule. The energies associated with such promotion of electron could be from non-bonding (n), or a π-orbital, to an antibonding π–orbital (π^*) or antibonding σ-orbital (σ^*). Lower the energy gap between the highest occupied molecular orbital (HOMO) and lowest unoccupied molecular orbital (LUMO), longer is the wavelength of light. Beer-Lambert

law tells us that fraction of incident radiation absorbed by a solute in a transparent solvent is independent of the intensity of incident light and is directly proportional to the concentration of absorbing molecules present in the solution at the fixed path length. Mathematically, this law is given by the following expression:

$$log\frac{I_0}{I} = A = \varepsilon cl \qquad (2.1)$$

Where, I_0 is the intensity of incident light

I is the intensity of transmitted light

A is absorbance

ε is molar extinction coefficient or molar absorptivity.

c is the concentration of solute

l is the cell path length (1cm)

That is, larger the number of molecules that absorb light of a given wavelength, greater is the extent of light absorption and higher the peak intensity in absorption spectrum. If there are only a few molecules that absorb radiation, the total absorption of energy is less and consequently lower intensity peak is observed.

Using this technique, the concentration of the adsorptive, reactants utilized and products formed can be determined in-situ in a dilute solution or reaction mixture. The absorption of incident radiation also takes place due to the localized surface plasmon resonance (LSPR) of the metal nanoparticles. LSPR absorption is characteristic of the

noble metal nanoparticles and also dependent on the nature of metal, stabilizer, size and shape of the nanoparticles.

2.6.2 Fourier Transform Infrared Spectroscopy (FT-IR)

Fourier transform-Infrared spectroscopic measurements were conducted on Varian 3100 FT-IR spectrometer. FT-IR spectroscopic analysis was carried out by mixing nanomaterial sample for measurement with KBr in agate pestle and mortar followed by pelletization. FT-IR spectra were recorded between spectral range 4000 and 400 cm^{-1}, with a resolution of 0.09 cm^{-1}.

Principle

Various molecular vibrational modes such as bond stretching or bending in molecules can be excited from lower vibrational energy states to higher vibrational states by absorbing IR radiations. All vibrational modes of bonds in a molecule are not capable of absorbing IR energy. Only those vibrational modes which are accompanied by change in the dipole moment of the molecules result in infrared active transitions. The vibrational energy change is also accompanied by a large number of rotational energy changes. Therefore, vibrational spectra appear as vibrational-rotational bands. In IR-spectroscopy, the absorbed energy brings about predominant changes in the vibrational energy and is dependent on, masses of atoms present in molecule, strength of bond and the arrangement of atoms within the molecule.

The FT-IR instrument consists of five components i.e. source, interferometer, sample holder, detector, data processing. Source gives radiation which covers the entire

spectral range to be measured. In every scan, all source radiation is passed through the interferometer and then gets to the sample. The interferometer consists of beam splitter, a fixed and movable mirror. The beam splitter is a plate made up of IR transparent material like KBr. This plate is coated in such a way that 50 % radiation is falling on it, is reflected and rest passes through (Figure 2.1). It splits the incoming radiation in two directions at right angles with one portion going to a stationary mirror then back to the beam splitter. The other half of the radiation goes to a moving mirror. The total path length due to the movable mirror is different from that traversed by the beam that comes from the stationary mirror. The difference in path lengths creates an interferogram when the two beams meet and recombine at the beam splitter. The recombined beam is passed through the sample, which absorbs the wavelengths characteristic of its spectrum. This process, therefore, subtracts specific wavelengths from the interferogram. The detector now reports variation in energy versus time for all wavelengths simultaneously. Fourier transformation of the data converts the intensity versus time spectrum into intensity versus frequency spectrum. In this thesis FTIR spectroscopy was used to identify the surface functional groups on the nanomaterials.

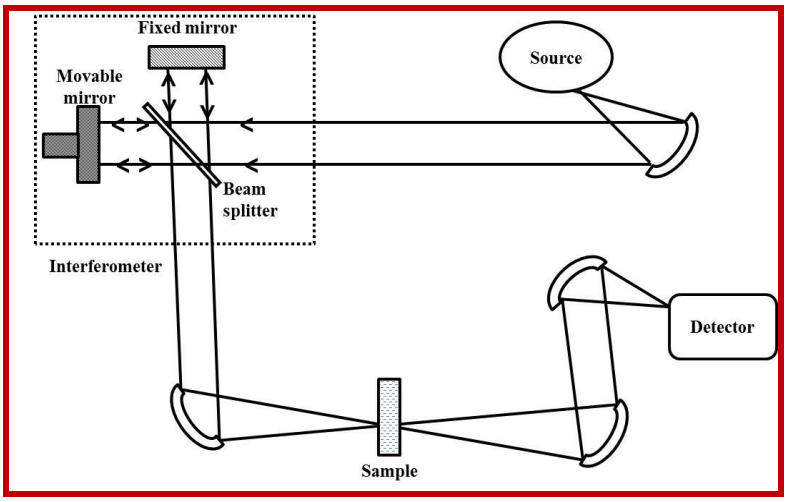

Figure 2.1 Schematic ray diagram of the working of FT-IR instrument.

2.6.3 Nuclear Magnetic Resonance Spectroscopy (NMR)

The NMR spectrum of the product was obtained using Bruker 500 MHz NMR spectrometer. The purified compound was dissolved in dimethyl sulfoxide (DMSO) and 500µL of this sample solution was taken in a NMR tube for measurement.

Principle

When a molecule is placed in a magnetic field, circulation of electrons results in the formation of secondary magnetic field i.e. induced magnetic field. Rotation of electron about the proton generates a field which opposes the applied field and the proton is said to be shielded. The rotation of electron about the nearby nuclei also generates a field that can either reinforce or oppose the applied field then the proton is said to be deshielded or shielded respectively. Such shifts in a position of NMR which arise due to shielding and deshielding of proton by the electron are called as chemical shift. Chemical shift is measured by taking tetramethylsilane (TMS) as a reference. The number of signals found in the NMR spectrum corresponds to the number of nonequivalent proton groups in the molecule. Position of signals (Chemical shift) in the spectrum helps us to know the nature

of proton such as aromatic, aliphatic, adjacent to some electron attracting or electron releasing groups, etc. Therefore depending upon the electronic environment they absorb at different applied field strengths.

NMR makes use of a radio-frequency, magnet, detector and an amplifier (Figure 2.2). The detection system is used to measure the amount of energy being transferred from the radio-frequency beam. The sample under investigation is taken in a glass tube and placed in between the poles faces of the magnet.

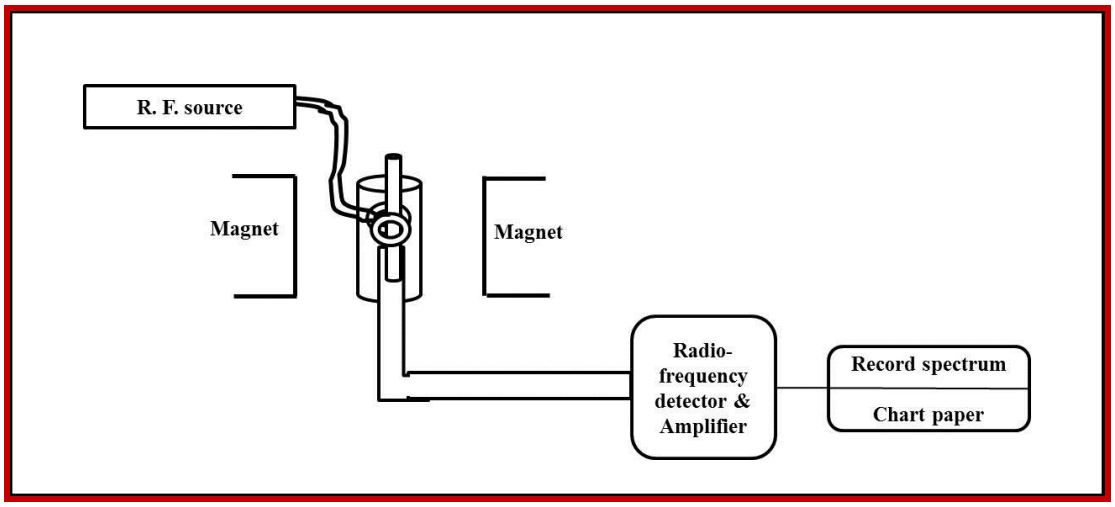

Figure 2.2 Schematic of components in NMR instrument.

A radio frequency source is made to fall on the sample. It is done by feeding radio frequency source into a coil around the sample tube. A signal is detected if the nuclei in the sample resonate with the source, the energy required to flip the proton is the same as that of the source. Energy is transferred from the source via nuclei to the detector. The output from the detector can be fed to a cathode ray oscillograph or to the strip chart recorder after amplification.

The information of the type of equivalent sets of protons with characteristic values of chemical shift helps in the elucidation of structure of the compound.

2.5.3. X-ray Diffraction

The X-ray diffraction spectra of nanomaterials prepared in this thesis were recorded using Mini Flex 600 (Rigaku, Tokyo, Japan) model. This instrument consists of the source (X ray generation), optics, goniometer and detector. The tube voltage and current utilized are 40 kV and 15 mA respectively. The optics consists of optional graphite monochromator, soller slit (5.0° or 2.5°), and fixed scattering slit. It has a vertical goniometer of radius 150 nm with accuracy of ± 0.02°. NaI scintillator and high speed silicon strip detector is present in Mini Flex 600. Instrument employing Cu-K_α radiation having wavelength (λ =1.54059 Å). For analysis of sample a thin layer of powdered nanomaterial sample was placed in a goniometer rotating at the rate of 1^0 per minute with step size of 0.02.

Principle

Incident X-ray interacts with material and undergoes diffraction from planes of atoms or molecules of a crystalline material. If the interplanar spacing (d) is an integer multiple of X ray wavelength, then the diffracted X-rays interfere constructively (Figure 2.3). Bragg's equation gives the linear correlation between wavelength and interplanar spacing of periodic solid powder. The Bragg's relation is expressed as

$$n\lambda = 2dsin\theta \qquad (2.2)$$

Here n is order of reflection i.e 1, 2, 3,……, λ represents wavelength of incident radiation, d is the interplanar spacing and θ is Bragg angle.

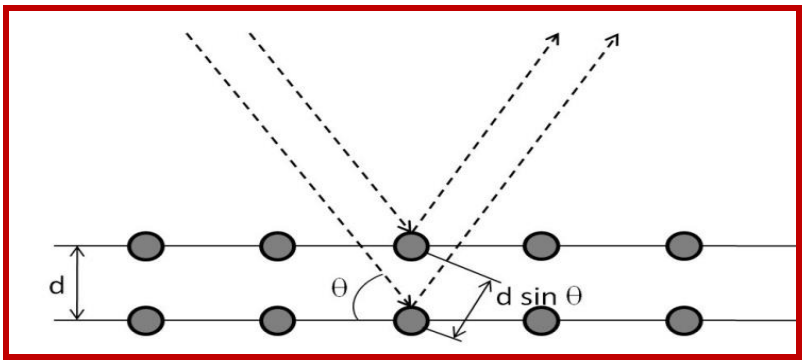

Figure 2.3 Schematics of Bragg Diffraction.

Peak broadening occurs when X-ray passes through sample having crystallite size 500 nm. Such broadening is further quantified by finding the full width half maximum (FWHM) from the diffraction pattern. The average crystallite size can be calculated by the Scherrer's formula given below

$$D = \frac{k\lambda}{\beta cos\theta} \qquad (2.3)$$

In this expression D is the coherently scattered domain size, k represents dimensionless constant (≈0.9), λ is wavelength, β indicates instrument corrected FWHM in radian and θ is diffraction angle. [Cullity *et al.* (2001), Battaut *et al.* (1962)].

This is a powerful technique for identifying crystalline phases, crystallite size, and strains in the materials.

2.5.4. Transmission electron microscopy

Transmission electron microscopy (TEM), FEI Technai-20 G^2 at operating voltage of 200 keV was used to record the TEM micrographs of prepared nanomaterials. Ag, Cu and Ag-Cu BNPs samples were re-dispersed in ethanol to a dilution of about 10 times to that required for sample prepared for UV-Vis absorption measurement. This solution was

sonicated for 30 min in water bath. One drop of this sonicated sample was dropped on carbon coated Cu grid (400 mesh size). The BNPs samples were prepared on carbon coated Ni grid of 200 mesh size. This grid was dried for 12 hours in vacuum desiccator before placing the specimen in a holder for microscopic investigations.

Principle

Transmission electron microscopy (TEM) is a microscopic imaging technique where a beam of high energy electron is focused onto a sample causing an enlarged version to appear on a fluorescent screen or layer of photographic film. TEM is capable of giving information both in real as well as in reciprocal space. Therefore, it gives morphological and structural information about specimen. The analytical version of TEM in particular in its scanning mode with energy dispersive spectroscopy (EDS) can reveal its elemental composition present in the material. Moreover, it provides a better understanding especially with respect to atomic resolution real spacing images of material at nanoscale [Wang et al. (2000)]. The image formed is magnified further to be detected by the sensor such as a CCD camera. TEM instrument consist of three important parts moving from top to bottom: (1) electron gun, (2) image producing system (3) image recording system. Electron gun is a cathode made up of tungsten or LaB6 which produces electron beam [Egorton *et al.* (2005)]. This electron gun is controlled by two factors first is filament current (controls the temperature of the filament and hence the number of electrons emitted to obtain a large number of electrons emitted from a small region of the filament). Second parameter is bias (potential controls the size of the region of filament and the main reason to alter bias is to change the brightness of the beam). Smaller the wavelength of the electron leads to the higher resolution although the quality of the image is

controlled by the lens system of TEM. The condenser lens controls the intensity and angular aperture of beam between the gun and the specimen. Single lens may help to converge the beam onto the object. But commonly, a double condenser lens is employed. In this the first lens is strong and produces a reduced image of the source, which is then imaged by the second lens onto the object. Such an arrangement gives an effective space between the electron gun and the object stage. It is more flexible as the reduction in size of the image of the source may be varied widely by controlling the first lens [Rose *et al.* (2008)]. The image is monochromatic and must be made visible to the eye by allowing the electrons to fall on a fluorescent screen fitted at the base of the microscope column. The image can also be captured digitally for display on a computer monitor. Computerized images are stored in a TIFF or JPEG format and analyzed. TEM utilized to find out the nature of phases formed and their microstructures.

2.5.5. High resolution scanning electron microscopy

FEI NOVA NANOSEM 450 model is used for recording SEM images. The dried powder sample was placed on a double sided tape which sticks to the sample holder.

Principle

The Scanning Electron Microscopy is widely used to examine the microscopic structure by scanning the surface of materials. It uses a focused beam of high-energy electrons (~30 kV) to generate a variety of signals at the surface of solid specimens. The signal that derives from electron and sample interaction reveals the information about the sample including external morphology by means of secondary and backscattered electrons, chemical composition with X-ray spectroscopy, and texture in the sample with electron backscattered diffraction.

2.5.6. Energy Dispersive X-ray Analysis (EDX)

EDX measurements were carried out by the use of FEI NOVA NANOSEM 450 having AMETEK detector. The sample is prepared as in the SEM imaging process.

Principle

Energy Dispersive X-Ray Spectroscopy is a micro analytical technique that can be coupled with Scanning Electron Microscopy (SEM). EDX combined with these imaging tools can provide elemental analysis on areas as small as nanometers in diameter. EDX utilizes the X-ray spectrum emitted by a solid sample bombarded with a focused beam of electrons to obtain the confined chemical analysis. Almost all elements from atomic number 4 to 92 are possible to measure. The impact of the electron beam on the sample produces X-rays that are characteristic of the elements present in the sample. When the SEM electron beam bombards the sample, electrons are ejected from the atoms available on the sample surface. The resulting electron vacancies are filled by electrons from a higher state generating the X-ray to balance the energy difference between the two electron states. The X-ray generated is the characteristic of the element from which it was emitted. This technique determines the elemental composition of individual points or maps out the adjacent distribution of elements from selected areas such as presence of one or more elements in the sample. Chemical composition and purity of Ag-Cu bimetallic nanoparticles were determined by EDX. SEM is also helpful in determining the size and shape of nanoparticles. Chemical compositions of elements in sample can be known with SEM-EDX facility.